Motional rotating-wave approximation for harmonically trapped particles

Özgür E. Müstecaplıoğlu and L. You

School of Physics, Georgia Institute of Technology, Atlanta, Georgia 30332-0430
(Received 21 June 2001; published 20 February 2002)

We present a family of generalized unitary transformations that simplifies the Hamiltonian for a harmonically trapped two-level atom (or ion) interacting with a plane wave laser field. Near-resonant single as well as double vibrational phonon dynamical regimes are found. The validity condition of the often used motional rotating-wave approximation (MRWA) is examined both numerically and analytically. Large errors are found within typical regimes of the MRWA with respect to the motional degrees of freedom. The effects of the MRWA in trapped ion systems are shown to be opposite to that of the rotating-wave approximation in the usual Jaynes-Cummings model. Our study points to a more restrictive condition on the particle localization (Lamb-Dicke) parameter for the validity of the MRWA in the single phonon dynamical regime. It also sheds light on quantum information storage and processing with trapped atoms.

I. INTRODUCTION

In the last few years, much attention has been focused on quantum dynamics and coherence properties of trapped atoms or ions [1–5]. These studies led to many potentially attractive applications of harmonically trapped particles, e.g., in generating nonclassical vibrational phonons [6], implementing fast quantum gates [2], and achieving phonon-ion entanglement [1]. In most of these studies, a coherent plane wave laser field near-resonantly couples two electronic states of an atom. The inclusion of motional degrees of freedom leads to tremendous complication. Several simplifications have been developed that reduce the trapped particle dynamics to the familiar Jaynes-Cummings model (JCM) form with the use of the Lamb-Dicke limit (LDL), the strong confinement limit, or the motional rotating wave approximation (MRWA). In fact, the JCM description can be achieved regardless of the laser field configuration, i.e., whether it is a traveling wave [3] or a standing wave [1,4]. The LDL requires the particle localization size, given by the harmonic trap ground state width a, to be much less than the near-resonant laser wavelength λ, i.e., $\eta = (2\pi)a/\lambda \ll 1$. It is often believed that the MRWA for harmonically trapped particles works well within the LDL as it demands a less restrictive condition $\eta \ll 2$ [3] or $\eta \ll 4$ [2].

In our ongoing effort to understand motional effects of trapped particles for quantum information processing [7], this issue of the validity regimes for the trapped particle MRWA again arises. We note that some earlier investigations show that the rotating-wave approximation (RWA) does not work satisfactorily for Hamiltonians containing multiple transitions [8,9] or for systems initially prepared in a superposition of internal states [10]. Furthermore, multiparticle properties such as entanglement can have a different sensitivity dependence on the single particle MRWA [11]. With harmonically trapped particles, this issue becomes particularly acute as the equal distant motional states span an infinite dimensional Hilbert space. The MRWA is typically made after a linearization by either taking the LDL or applying an exact simplifying unitary transformation. Within the latter approach, errors from the MRWA can be further modified by

the back transformation when dynamical observables are calculated in the original frame.

In this article we study the quantum dynamics of a single trapped atom by employing a numerical diagonalization procedure without employing the MRWA. We assess the validity regime for the MRWA by comparing with results from analytical models obtained under the MRWA. This paper is organized as follows. In Sec. II, our model system of a single trapped two-level atom is described and a review of the unitary transformation method for linearizing the Hamiltonian is presented. Our result, the existence of a family of general unitary transformations for linearizing our model Hamiltonian, is then introduced. In Sec. III, we discuss two linearized models obtainable from our transformations. In Sec. IV, we outline several technical points about analytical solutions of the transformed model Hamiltonian under the MRWA. We also discuss a numerical diagonalization procedure used for exact dynamic solutions. Selected results and comparisons are presented in Sec. V. Finally, we conclude in Sec. VI.

II. THE MODEL SYSTEM AND A FAMILY OF GENERAL UNITARY TRANSFORMATIONS

To simplify our discussion, we consider a one-dimensional model of a harmonically trapped two-level particle interacting with a near-resonant laser field [3,12]. The system Hamiltonian is given by

$$\mathcal{H} = \mathcal{H}_0 + \mathcal{H}_1,$$

$$\mathcal{H}_0 = \frac{P^2}{2M} + V_{tg}(x)\sigma_{gg} + [\hbar\omega_{eg} + V_{te}(x)]\sigma_{ee},$$

$$\mathcal{H}_1 = \frac{\Omega}{2} e^{i\hbar\omega_L t} e^{-ik_L x}\sigma_- + \text{H.c.}, \tag{1}$$

where Ω, ω_L, and k_L denote, respectively, the Rabi frequency, carrier frequency, and wave number of a coherent driving laser. The electron transition frequency between the excited ($|e\rangle$) and ground states ($|g\rangle$) is ω_{eg}. $\sigma_{ab} = |a\rangle\langle b|$ ($a/b = e, g$) are atomic projection operators. Consistently

with convention, we denote $\sigma_- = |g\rangle\langle e|$ and $\sigma_z = \sigma_{ee} - \sigma_{gg}$. For a neutral particle, typically the approximate harmonic trap potential is internal state dependent, i.e., $V_{ta} = (1/2)M\nu_a^2 x^2$ with a corresponding trap frequency ν_a. P is the motional momentum and M is the mass of the particle.

We first simplify Eq. (1) by changing into the interaction picture (rotating frame) with the unitary transformation $\mathcal{H} \rightarrow e^{i\hbar \omega_L t \, \sigma_{ee}} \mathcal{H} e^{-i\hbar \omega_L t \, \sigma_{ee}} - \hbar\omega_L \sigma_{ee}$. This leads to

$$\mathcal{H}_0 = \frac{P^2}{2M} + V_{tg}(x) + \frac{\hbar\delta}{2}\sigma_z + [V_{te}(x) - V_{tg}(x)]\sigma_{ee} + \frac{\hbar\delta}{2},$$

$$\mathcal{H}_1 = \frac{\Omega}{2} e^{-ik_L x}\sigma_- + \text{H.c.}, \qquad (2)$$

where $\delta = \omega_{eg} - \omega_L$ is the laser field detuning. We now introduce the motional phonon annihilation (creation) operator for the ground state a ($a^\dagger$) according to $P = \sqrt{\hbar M \nu_g / 2}\, p$ and $x = \sqrt{\hbar/2M\nu_g}\, q$ with $p = i(a^\dagger - a)$ and $q = a^\dagger + a$. The displacement operator becomes $D(\beta) = e^{\beta a^\dagger - \beta^* a}$, and Eq. (2) simplifies to ($\hbar = 1$)

$$\mathcal{H}_0 = \nu_g n + \frac{\delta}{2}\sigma_z + \zeta q^2 \sigma_{ee} + \frac{\nu_g + \delta}{2},$$

$$\mathcal{H}_1 = \frac{\Omega}{2} D^\dagger(i\eta)\sigma_- + \text{H.c.}, \qquad (3)$$

where $n = a^\dagger a$ is the phonon number operator and $\zeta = (\nu_e^2 - \nu_g^2)/4\nu_g$. The Lamb-Dicke parameter is now $\eta = k_L\sqrt{1/2M\nu_g}$. For this particular form of the Hamiltonian, we note that its interaction part ($\mathcal{H}_1$) can be diagonalized by a general transformation matrix $\tilde{T} = E^\dagger T$, with

$$E = \frac{E_2 + E_1}{2}\hat{I} + \frac{E_2 - E_1}{2}\sigma_z,$$

$$T = \frac{1}{\sqrt{2}}\left(\frac{D^\dagger(i\eta) + 1}{2}\hat{I} + \frac{D^\dagger(i\eta) - 1}{2}\sigma_z + \sigma_+ - D^\dagger(i\eta)\sigma_-\right). \qquad (4)$$

We choose $\Omega \in \mathfrak{R}$ without loss of generality. It is easy to check that $\tilde{T}\mathcal{H}_1\tilde{T}^\dagger = (\Omega/2)\sigma_z$, is independent of the arbitrary unitary functional operators $E_{1,2}$ of a and $a^\dagger$. For any operator Θ, the transformed operator will be denoted by $\bar{\Theta} = \tilde{T}\Theta\tilde{T}^\dagger$. $\hat{I} = \sigma_{ee} + \sigma_{gg}$ is the identity operator. This transformation can be compared to the generalized Power-Zienau transformation discussed earlier [13]. In the phonon Fock state basis, it generates coherent superpositions of motional wave-packet states which were previously used in studying motional decoherence of atomic qubit operations [7]. It reduces to the simplifying transformation used by Moya-Cessa et al. [3] when we take $E_1 = E_2 = D(-i\eta/2)$. The $\tilde{T}$ transformation on the $\mathcal{H}_0$ term can be conveniently calculated using the following properties:

$$D(\alpha)D(\beta) = e^{(\alpha\beta^* - \alpha^*\beta)/2}D(\alpha + \beta), \qquad (5)$$

$$D(\mp i\eta)a^\dagger a D(\pm i\eta) = a^\dagger a \pm i\eta(a^\dagger - a) + \eta^2, \qquad (6)$$

for arbitrary complex numbers α and β. We note that Eq. (5) simplifies to $D(\alpha)D(\beta) = D(\alpha + \beta)$ when α and β are purely imaginary. The second and the last terms in the right-hand side of Eq. (6) correspond to the Doppler and recoil shifts. After this general transformation, we obtain

$$\tilde{\mathcal{H}}_0 = E^\dagger\left[\left(\nu_g n + gp + \eta g + \frac{\delta + \nu_g}{2} + \frac{\zeta}{2}q^2\right)\hat{I} - \left(gp + \frac{\zeta}{2}q^2 + \eta g + \frac{\delta}{2}\right)\sigma_x\right]E, \qquad (7)$$

with $g = \eta\nu_g/2$ and $\sigma_x = \sigma_+ + \sigma_-$. Different simplifications can be pursued by exploiting other forms of $E_{1,2}$. We note that the first term in Eq. (7) is in the form of a squeezed displaced harmonic oscillator. Therefore it can be diagonalized in the Fock state basis by the squeezed coherent state transformation $E_2 = E_1 = D(\beta)S(\xi)$. To eliminate the p dependence in the coefficient of $\hat{I}$ we choose $\beta = -i\eta/2$, which transforms according to $n \rightarrow n - (\eta/2)p + \eta^2/4$, $p \rightarrow p - \eta$, and $q \rightarrow q$. We then obtain

$$\tilde{\mathcal{H}}_0 = S^\dagger(\xi)\left[\left(\nu_g n + \frac{\zeta}{2}q^2 + \frac{\delta + \nu_g + \eta g}{2}\right)\hat{I} - \left(gp + \frac{\zeta}{2}q^2 + \frac{\delta}{2}\right)\sigma_x\right]S(\xi). \qquad (8)$$

The squeezing transformation $S(\xi = re^{i\theta})$ causes $a \rightarrow ua^\dagger - v^*a$ with $u = \cosh r$ and $v = e^{i\theta}\sinh r$. For our model, ζ is required to be real, i.e., $\theta = 0$. The action of S results in

$$p \rightarrow e^r p,$$

$$q \rightarrow e^{-r} q,$$

$$n \rightarrow e^{2r}n - \frac{1}{2}\sinh 2r\, q^2 + e^r \sinh r. \qquad (9)$$

Substitution of these results into Eq. (8) leads to the elimination of the q^2 term in the coefficient of the $\hat{I}$ term provided we choose $r = (\ln\epsilon)/4$ with $\epsilon = 1 + 2\zeta/\nu_g$. This yields

$$\tilde{\mathcal{H}}_0 = \left[\nu_g\sqrt{\epsilon}\, n + \frac{\nu_g\sqrt{\epsilon} + g\eta + \delta}{2}\right]\hat{I} - \left(g\epsilon^{1/4}p + \frac{\zeta}{2\sqrt{\epsilon}}q^2 + \frac{\delta}{2}\right)\sigma_x. \qquad (10)$$

We can now redefine the parameters according to $\nu = \nu_g\sqrt{\epsilon}$, $g \rightarrow g\epsilon^{1/4}$ and $\zeta \rightarrow \zeta/\sqrt{\epsilon}$. Finally, we arrive at the transformed Hamiltonian

$$\tilde{\mathcal{H}} = \nu n + \frac{\Omega}{2}\sigma_z - \left(gp + \frac{\zeta}{2}q^2 + \frac{\delta}{2}\right)\sigma_x, \qquad (11)$$

where the constant term in the coefficient of $\hat{I}$ has been dropped. We note that for ions with internal state independent trap frequencies $\zeta = r = \xi = 0$. We recover the same result as in Ref. [3] by choosing $\beta = -i\eta/2$. The effects of different trap frequencies for different internal levels are a renormalization of energy parameters in the single vibrational phonon Hamiltonian and a double vibrational phonon interaction through a term quadratic in the position operator. Double phonon transitions are the typical interactions that can lead to squeezed and entangled states for the vibrational phonons. In the next section, we will see that such two-phonon transitions can dominate the single phonon transitions in the system, independent of the Lamb-Dicke parameter η.

III. MOTIONAL ROTATING-WAVE APPROXIMATION

The simplified model Hamiltonian Eq. (11) is of the form of a generalized JCM involving quadratic two-phonon transitions. It can be analytically solved for small squeezing parameters without external drive ($\Omega = 0$) [14]. Alternatively, when $|\nu - \Omega| \ll \Omega$ or $|2\nu - \Omega| \ll \Omega$, and g and $\zeta \ll \Omega$, an approximate analytic solution can be obtained by an explicit diagonalization upon the elimination of the rapidly oscillating terms, i.e., the application of the MRWA. In the interaction picture, Eq. (11) becomes

$$\widetilde{\mathcal{H}}_I = \left[-ig(a^\dagger e^{i\nu t} - a e^{-i\nu t}) + \frac{\zeta}{2}(a^{\dagger 2} e^{i2\nu t} + a^\dagger a + \text{H.c.}) + \frac{\delta}{2} \right]$$
$$\times (\sigma_+ e^{i\Omega t} + \sigma_- e^{-i\Omega t}). \tag{12}$$

There exist two resonance conditions, one at $\Omega = \nu$ where the validity condition for the MRWA becomes $(\eta \nu_g/2)\epsilon^{1/4} \ll \nu_g \epsilon^{1/2}$ [14], i.e., $\eta \ll 2\epsilon^{1/4}$. When the difference in trap frequencies is small we get $\eta \ll 7/4 + (\nu_e/2\nu_g)^2$. We see that the validity regime of the MRWA depends on η for this case of the single phonon JCM. Physically, the trap frequency difference can be controlled experimentally [15]. When $\nu_e = \nu_g$ as for an ion, we recover the condition $\eta \ll 2$ as discussed by Moya-Cessa *et al.* [3]. Under this condition, we arrive at the single phonon model:

$$\widetilde{\mathcal{H}}_{\text{MRWA}}^{(1p)} = \mathcal{H}_{\text{free}}^{(1p)} + V^{(1p)},$$

$$\mathcal{H}_{\text{free}}^{(1p)} = \nu a^\dagger a + \frac{\nu}{2} \sigma_z,$$

$$V^{(1p)} = -ig(a^\dagger \sigma_- - a\sigma_+). \tag{13}$$

This Hamiltonian is the same as in the Jaynes-Cummings model $H_{\text{JCM}} = \nu a^\dagger a + (\nu/2)\sigma_z - gp\sigma_x$ with the counter-rotating terms $a^\dagger \sigma_+, a\sigma_-$ dropped under the RWA.

Alternatively, there is a second resonance at $\Omega = 2\nu$. The condition for the MRWA in this case is $\zeta/2 \ll \Omega$ [16], which becomes $7\nu_e^2 + 9\nu_g^2 \gg 0$. Hence, the validity regime of the MRWA becomes independent of η in this case and can be realized simply by choosing larger trap frequencies. In contrast to the single phonon JCM in Eq. (13), the two-phonon squeezing model can be achieved beyond the LDL and is described by

$$\widetilde{\mathcal{H}}_{\text{MRWA}}^{(2p)} = \mathcal{H}_{\text{free}}^{(2p)} + V^{(2p)},$$

$$\mathcal{H}_{\text{free}}^{(2p)} = \nu a^\dagger a + \nu \sigma_z,$$

$$V^{(2p)} = \frac{\zeta}{2}(a^{\dagger 2}\sigma_- + a^2 \sigma_+). \tag{14}$$

Equations (13) and (14) are the major results of the general unitary transform introduced earlier. Their complete dynamics, however, can be complicated as transformation back into the original Schrödinger picture induces coherent mixing of different states. In particular, if the system is initially prepared in a state $\psi(0)$, the linearized model Hamiltonian, Eq. (13), has an initial state $\widetilde{\psi}(0) = T\psi(0)$, which is always a superposition of both internal states. In other words, even for systems initially in only one internal state such that it has a vanishing dipole moment, the transformed system will always have a nonvanishing dipole moment. It is known in this case that counter-rotating terms (CRT's) neglected in making the MRWA become more significant and the validity regimes for the MRWA more restricted [10].

We are now in a position to discuss the validity regimes of the commonly used MRWA for the simplified model Hamiltonians Eqs. (13) and (14). We will focus on the single phonon model in Eq. (13) as it can be compared directly to existing results (under the MRWA) in the literature [3]. Furthermore, while the single phonon JCM can be obtained for small restricted values of the Lamb-Dicke parameter, the two-phonon model is obtained without any restriction on the Lamb-Dicke parameter. Thus, determining the validity regime of the MRWA is more essential for the single phonon JCM.

IV. NUMERICAL METHOD

In the following discussion we focus on the single phonon model and thus ignore the unnecessary superscript (1p) for notational simplicity. In the numerical studies, for the approximate JCM Eq. (13) we propagate any given initial states according to $\widetilde{\psi}(t) = e^{-i\mathcal{H}_{\text{free}}t} U_I(t) \widetilde{\psi}(0)$ with the known propagator $U_I(t) = e^{-itV}$ in the interaction picture [17],

$$U_I(t) = \frac{1}{\sqrt{2}} \begin{pmatrix} \cos[gt\sqrt{aa^\dagger}] & \sin[gt\sqrt{aa^\dagger}]\dfrac{a}{\sqrt{aa^\dagger}} \\ -\dfrac{a^\dagger}{\sqrt{aa^\dagger}}\sin[gt\sqrt{aa^\dagger}] & \cos[gt\sqrt{a^\dagger a}] \end{pmatrix}. \tag{15}$$

Transformed states are denoted by $\widetilde{\psi} = \widetilde{T}\psi$. In the Schrödinger picture, where observables are computed, the wave function becomes $\psi(t) = \widetilde{T}^\dagger e^{-i\mathcal{H}_{\text{free}}t} U_I(t) \widetilde{T}\psi(0)$. For example, the mean phonon number $\langle a^\dagger a \rangle$ is found to be

$$\langle n \rangle = \psi(0)^\dagger \tilde{T}^\dagger U_I^\dagger e^{i\mathcal{H}_{\text{free}}t} \tilde{T} a^\dagger a \tilde{T}^\dagger e^{-i\mathcal{H}_{\text{free}}t} U_I(t) \tilde{T}\psi(0), \tag{16}$$

which can be further simplified with the use of the displacement operator property

$$\tilde{T} a^\dagger a \tilde{T}^\dagger = \left(a^\dagger a + \frac{\eta^2}{2}\right)\hat{I} - i\frac{\eta}{2}(a^\dagger - a)\sigma_x. \tag{17}$$

We note that the last term in the above equation involves the momentum operator. Therefore, it does not commute with $\mathcal{H}_0$ and introduces fast oscillations due to the $e^{-i2\nu t}$ factor. We finally get

$$\langle n \rangle = \tilde{\psi}(0)^\dagger U_I^\dagger \left[\left(a^\dagger a + \frac{\eta^2}{2}\right)\hat{I} - i\frac{\eta}{2}(a^\dagger e^{i\nu t} - ae^{-i\nu t})\right.$$

$$\left. \times (\sigma_+ e^{i\Omega t} + \sigma_- e^{-i\Omega t})\right] U_I \tilde{\psi}(0). \tag{18}$$

We immediately see that CRT's contribute to the dynamics of $\langle n \rangle$ because of multiple transitions in the original Hamiltonian. In addition to $\langle n \rangle$, CRT's also affect other dynamical variables of interest, e.g., the Mandel Q factor $[\langle (a^\dagger a)^2 \rangle - \langle a^\dagger a \rangle^2]/2$, which characterizes phonon statistics and the impurity factor $\mathcal{I} = 1 - \text{tr}(\rho_p^2)$ [18]. ρ_p is the reduced density operator in the phonon subsystem.

When all CRT's are included, i.e., no MRWA is made, it is no longer possible to solve the dynamic propagation analytically. However, the transformed Hamiltonian can be diagonalized numerically in a truncated phonon Fock state basis. It is easy to check the accuracy of such a truncation by testing for convergence with successively larger basis states. For an initial Poisson distribution of vibrational phonons, the dimension of the truncated space becomes small enough that efficient algorithms are readily available. To illustrate this, let us consider an initial state where the particle is in the internal state $|e\rangle$ with a motional coherent state $|\alpha\rangle$, i.e., $\psi(0) = |e\rangle|\alpha\rangle$. The transformed initial condition becomes

$$\tilde{\psi}(0) = e^{-i\eta\,\text{Re}(\alpha)}\frac{|e\rangle - |g\rangle}{\sqrt{2}}\left|\alpha - i\frac{\eta}{2}\right\rangle. \tag{19}$$

In a truncated Fock space of dimension N $(\gg |\alpha - i\eta/2|^2)$, the state vector is expanded as

$$\tilde{\psi}(t) = \sum_{n=1,\Lambda=e,g}^{N} X_{n+n_\Lambda}(t)|\Lambda n\rangle, \tag{20}$$

with $n_\Lambda = 0, N$ and $\Lambda = e, g$, respectively. The initial condition (19) then becomes

$$X_{n+n_\Lambda}(0) = s_\Lambda \frac{1}{\sqrt{2}} e^{-i\eta\,\text{Re}(\alpha)} F_{n-1}\left(\alpha - i\frac{\eta}{2}\right), \tag{21}$$

with $s_\Lambda = +1, -1$. The coherent state probability amplitudes in Fock space are $F_n(\alpha) = \exp(-|\alpha|^2/2)\alpha^n/\sqrt{n!}$. After back transformation, the original state vector evolution is then determined by

$$\psi(t) = \sum_{n=1,\Lambda=e,g} A_{n+n_\Lambda}(t)|\Lambda n\rangle, \tag{22}$$

with coefficients A_j for $(j=1,2,\ldots,2N)$ given by

$$A_{n+n_\Lambda}(t) = \frac{1}{\sqrt{2}} \sum_{m=1}^{N} D_{n-1,m-1}\left(s_\Lambda \frac{\eta}{2}\right)[X_m(t) + s_\Lambda X_{m+N}(t)]. \tag{23}$$

The displacement operator matrix elements in the Fock basis are known analytically in terms of Laguerre polynomials [19]. Therefore, the complete time evolution is obtained provided the transformed Hamiltonian is diagonalized. This is achieved through the standard expression

$$X_{i=1,\ldots,N}(t) = \sum_{j,k=1}^{2N} V_{ij}V_{jk}^{-1}e^{-iW_jt}X_k(0), \tag{24}$$

where W_j are the eigenvalues of the transformed Hamiltonian and V is the diagonalizing matrix whose columns are the corresponding eigenvectors. In the following section we will compare MRWA results with the numerical diagonalization method (NDM).
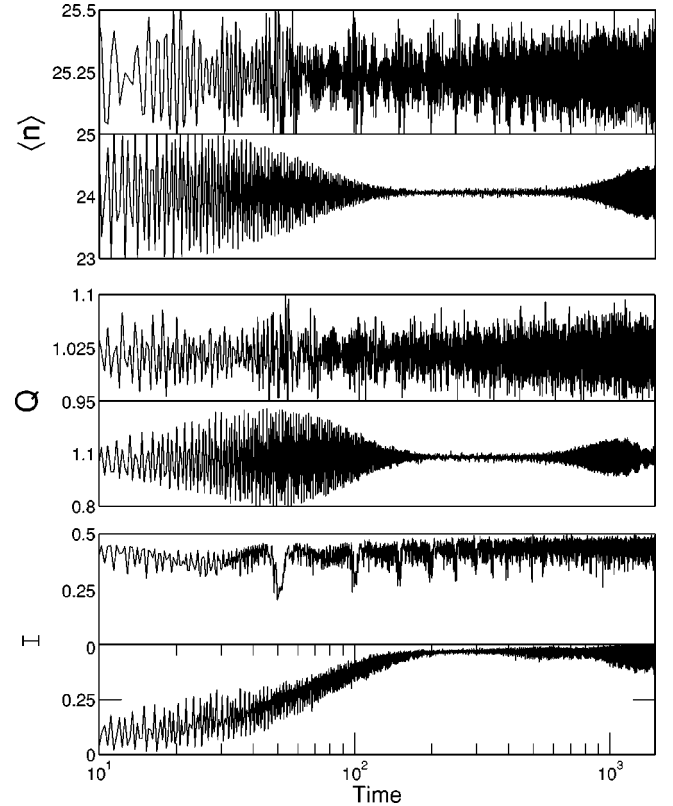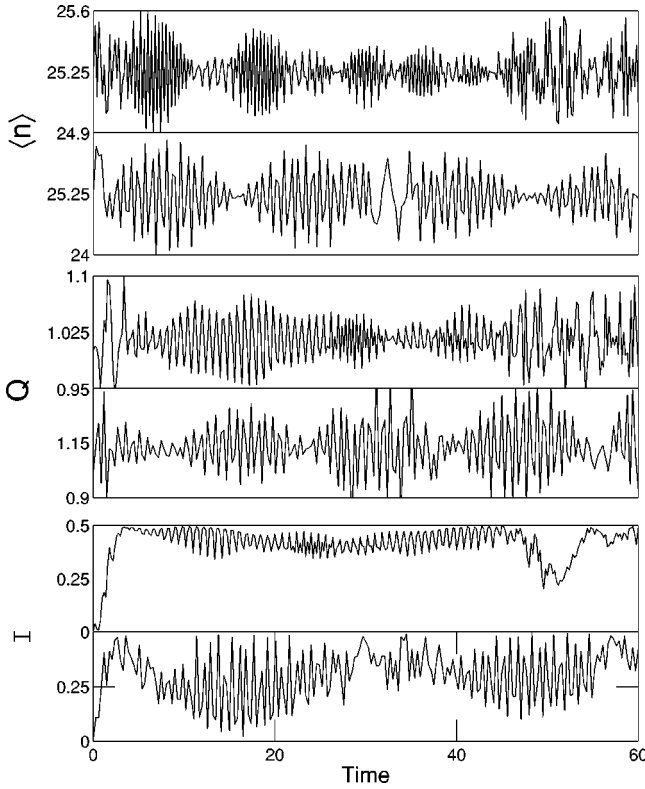

FIG. 1. Comparison of the mean phonon number $\langle n \rangle$, the Mandel Q factor, and the impurity parameter $\mathcal{I}$ for $\eta = 0.5$ and $\alpha = (0.5, 5)$. Always, the upper subfigures are from the exact numerical diagonalization, while the lower ones are from the MRWA. The time axis is in dimensionless form (scaled by $g = \eta\nu/2$). Note the differences as compared with Ref. [3].
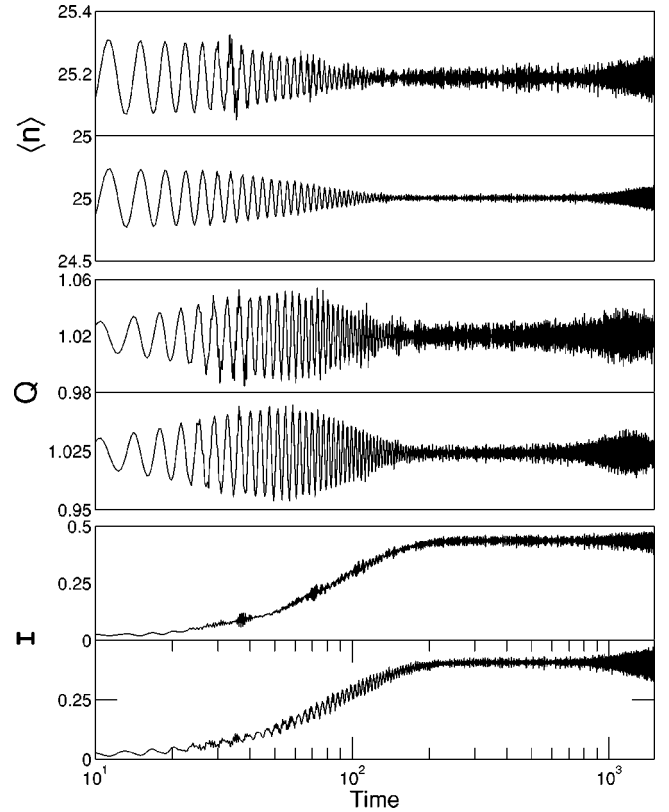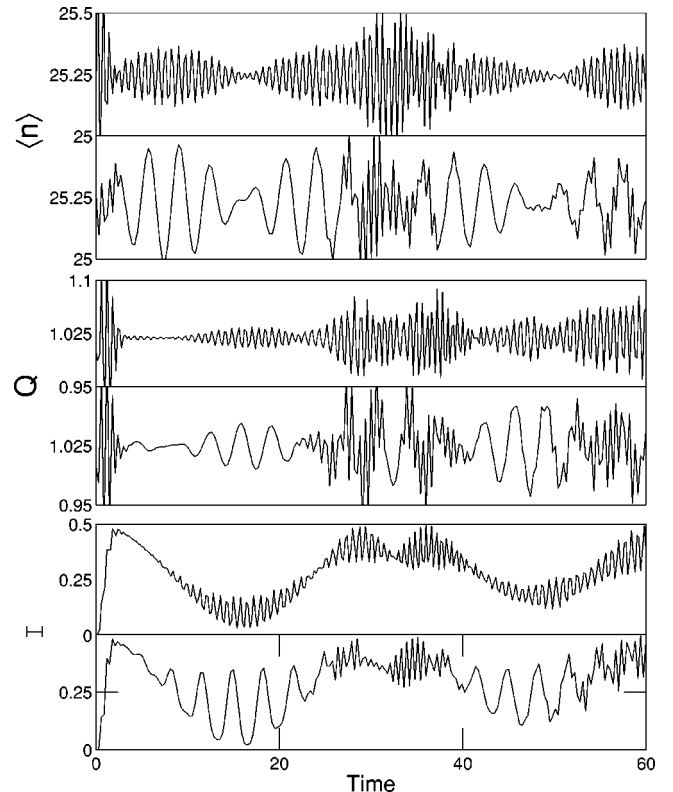
FIG. 2. The same as in Fig. 1 but for $\eta = 0.5$ and $\alpha = (5, 0.5)$.

V. RESULTS AND DISCUSSIONS

We focus in this section on the comparison of exact numerical results with results from the MRWA for an initial motional coherent state $|\alpha\rangle$ with $\alpha = |\alpha| \exp(i\beta)$. Moya-Cessa *et al.* [3] have discussed a restricted form of the unitary transformation that led to a similar linearized model Hamiltonian earlier. Although formally independent of the Lamb-Dicke parameter, their results were obtained under the MRWA. In this first example, we demonstrate that their illustrative figure as presented in Ref. [3] is in fact invalid at the presumed marginal LDL $\eta = 0.5$. In Fig. 1, we see that the MRWA result predicts regular behaviors for several dynamical variables, while the exact result from the NDM at $\eta = 0.5$ and $\alpha = (0.5, 5)$ displays significant differences. In general, we find that with the NDM the initial state loses its purity faster and ends up with a larger value for the time averaged mean phonon number. On the other hand, the MRWA results typically give larger widths of temporal fluctuations for the Mandel Q factor, especially at earlier times. Perhaps most importantly, the MRWA results predict super-revivals [3] in Q and $\langle n \rangle$ that were never observed with the NDM.

Differences of similar orders of magnitude are also found for $\alpha = (5, 0.5)$ as detailed in Fig. 2. We also note the significantly improved quantitative agreement for $\langle n \rangle$ in this case. In fact, such improved agreement with MRWA results always seems to occur when $\beta \approx 0$.

Now we compare the deeper LDL regime of $\eta = 0.1$. As shown in Figs. 3 and 4, noticeable errors with the MRWA

FIG. 3. The same as in Fig. 1 but for $\eta = 0.1$ and $\alpha = (0.5, 5)$. Note the super-revivals for Q.

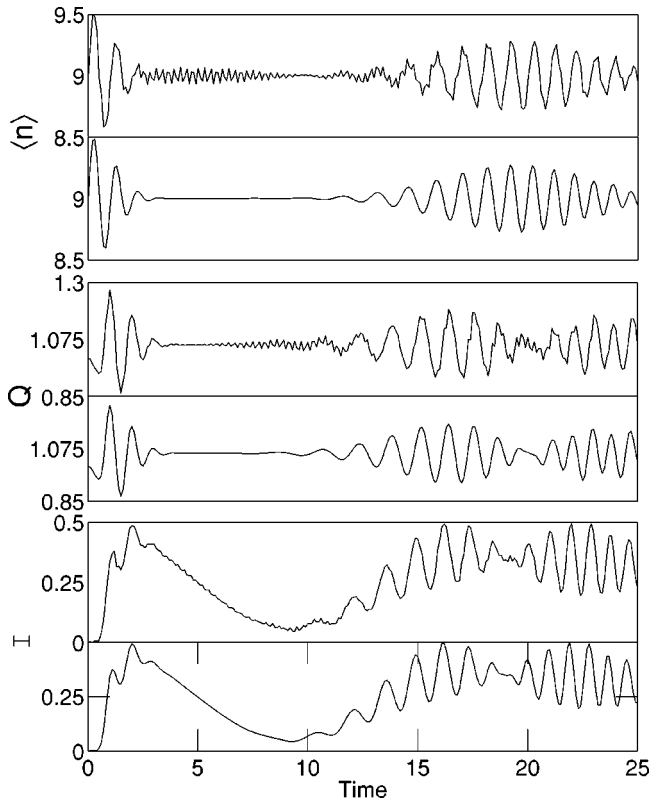FIG. 4. The same as in Fig. 1 but for $\eta = 0.1$ and $\alpha = (5, 0.5)$.

FIG. 5. The mean phonon number $\langle n \rangle$, the Mandel Q factor, and the impurity parameter $\mathcal{I}$ with $\eta = 0.1$ and $\alpha = (3,0)$ for the simple single phonon JCM H_{JCM} with and without the RWA. In both cases no back transformation is employed but an initial condition of the form $\tilde{T}\psi(0)$ is used to compare with the multiple phonon transition effects in Fig. 6. Within each subfigure, the upper (lower) part is for H_{JCM} with (without) counter-rotating terms.

were still found, although at significantly reduced levels as compared with Figs. 1 and 2.

Figure 4 compares early time dynamics for the same $\eta = 0.1$ but with $\alpha = (5, 0.5)$. We note that the $\mathcal{I} = 0$ value predicts the existence of Schrödinger cat states from both MRWA and NDM results [18]. Also the agreement for $\langle n \rangle$ and Q is better than the case of $\alpha = (0.5, 5)$. These results show clearly that errors in the MRWA are sensitive to the phase of the initial coherent state amplitude.

To further elucidate the effects of the MRWA, we have carried out additional comparisons. In Fig. 2 and in Fig. 4, we notice that the MRWA results predict larger oscillations than the actually smoother behavior of $\langle n \rangle$, Q, and I. This observation is in contrast to our expectations that stem from the effects of the RWA in the usual JCM. Let us first recall the effect of neglecting counter-rotating terms in H_{JCM}. For comparison, we consider an initial condition of the form $\tilde{T}\psi(0)$. The results obtained by propagating this initial condition under H_{JCM} dynamically with and without counter-rotating terms are given in Fig. 5. We see that results for H_{JCM} with the RWA exhibit smoother behavior while the actual H_{JCM} results carry small nutations due to counter-rotating effects. For the ion-trap system considered in Fig. 6, the results are just the opposite. In the ion-trap Hamiltonian,
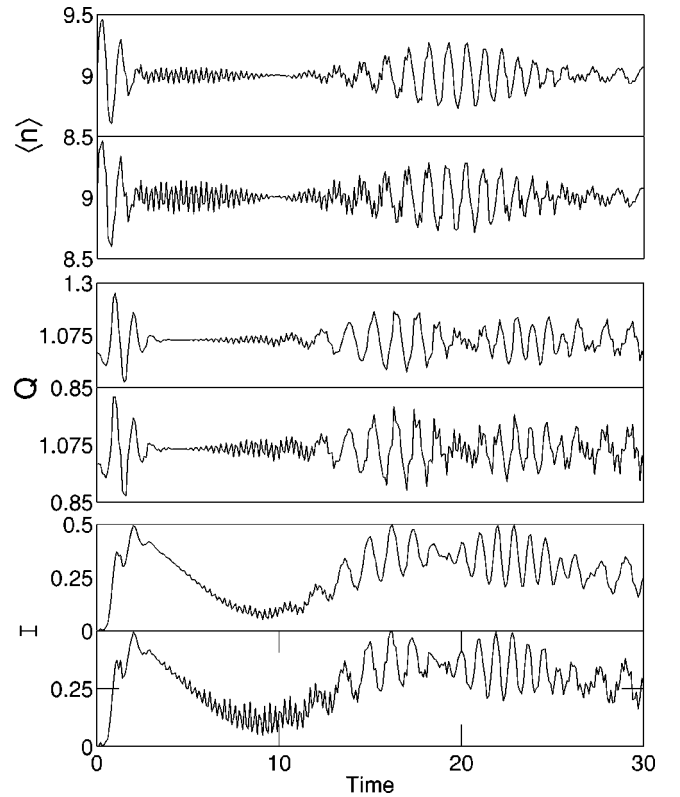

FIG. 6. The same as in Fig. 5 but now for the full ion-trap Hamiltonian which includes multiple phonon transition effects. Within each subfigure, the upper (lower) curve, obtained by the NDM (MRWA), is for the Hamiltonian with (without) counter-rotating terms.

the MRWA introduces more nutations in the actually smoother behavior. The basic difference between the JCM and the ion-trap system is the requirement of an additional back transformation for the latter, via $\tilde{T}^{\dagger}$ in determining the wave function evolution. From the physical point of view, this transformation brings back the effect of multiple phonon transitions, present in the ion-trap case, after a simplified single phonon transition dynamics has been determined conveniently in the interaction picture. Neglecting counter-rotating terms in the effective single phonon model Eq. (13), however, ignores too many multiple phonon processes at the end of the transformation, thus introducing more noise around the otherwise smoother collapse-revival patterns. We note that this (the MRWA in ion-trap models) is opposite to the effects of the RWA in the JCM and has been found for initial motional states with almost real coherent state amplitudes, i.e., $\beta \approx 0$.

VI. CONCLUSION

We have investigated the regimes of validity for the MRWA of a trapped particle under its coherent interaction with a plane wave laser field. Our study is based on a family of general unitary transformations that incorporate several earlier transforms as special cases [3,7]. This general transformation facilitates the linearization of the system Hamiltonian including the particle's motional degrees of freedom.

In model studies presented here, two distinct dynamical regimes appear, the single phonon dynamics and the double phonon dynamics. The single phonon model is standard in the deep LDL. The two-phonon model, on the other hand, does not impose any restrictions on the Lamb-Dicke parameter. Thus, addressing the validity regimes of the MRWA is necessary only for the single-phonon dynamics used extensively in the literature. For this aim, we have employed a numerical diagonalization procedure (without the MRWA) and comparatively assessed the validity conditions of the MRWA. We find that remarkable errors exist in regimes where the MRWA was believed to be applicable. Furthermore, our simulations show that the accuracy and detailed quantitative effects of the MRWA depend on the phase of the initial motional coherent state. When this phase is close to zero, the time averaged mean phonon number $\langle n \rangle$ displays improved agreement with MRWA results. The agreement, however, is far from perfect even in the deep LDL. Qualitatively, for almost real initial coherent state amplitudes, keeping the counter-rotating terms in the ion-trap model leads to smoother dynamical behaviors than the results obtained under the MRWA, which introduces larger nutations around the otherwise smoother dynamical patterns. This is in stark contrast to CRT effects in the usual JCM problems. Physically, this effect arises because of the existence of multiple transitions in motional states. Our study indicates that the connection between cavity QED and ion-trap systems in JCM-type formalisms is possible as long as the ranges of the Lamb-Dicke parameter are carefully analyzed to enforce the validity of the MRWA.

[1] M. Fang, S. Swain, and P. Zhou, Phys. Rev. A **63**, 013812 (2001).

[2] D. Jonathan, M.B. Plenio, and P.L. Knight, Phys. Rev. A **62**, 042307 (2000).

[3] H. Moya-Cessa, A. Vidiella-Barranco, J.A. Roversi, D.S. Freitas, and S.M. Dutra, Phys. Rev. A **59**, 2518 (1999).

[4] Y. Wu and X. Yang, Phys. Rev. Lett. **78**, 3086 (1997).

[5] S. Mancini, H. Moya-Cessa, and P. Tombesi, J. Mod. Opt. **47**, 2133 (2000).

[6] J.I. Cirac, A.S. Parkins, R. Blatt, and P. Zoller, Adv. At., Mol., Opt. Phys. **37**, 237 (1996).

[7] L. You, Phys. Rev. A **64**, 012302 (2001).

[8] E.A. Tur, Opt. Spectrosc. **89**, 574 (2000).

[9] M.F. Fang and P. Zhou, J. Mod. Opt. **42**, 1199 (1995).

[10] J. Seke, Nuovo Cimento Soc. Ital. Fis., D **16**, 303 (1994).

[11] R.H. Xie, Q. Rao, D.H. Liu, and G.O. Xu, Nuovo Cimento Soc. Ital. Fis., D **18**, 405 (1996).

[12] M. Lewenstein, L. You, J. Cooper, and K. Burnett, Phys. Rev. A **50**, 2207 (1994).

[13] P. Drummond, Phys. Rev. A **35**, 4253 (1987).

[14] C. Cohen-Tannoudji, J. Dupont-Roc, and G. Grynberg, *Atom-Photon Interactions* (John Wiley and Sons, Inc., New York, 1992).

[15] J. Ye *et al.*, Phys. Rev. Lett. **83**, 4987 (1999); D.W. Vernooy and H.J. Kimble, Phys. Rev. A **56**, 4287 (1997).

[16] J.S. Peng and G.X. Li, Phys. Rev. A **47**, 3167 (1993); K. Zaheer and M.S. Zubairy, *ibid.* **37**, 1628 (1988).

[17] M.O. Scully and M.S. Zubairy, *Quantum Optics* (Cambridge University Press, New York, 1997).

[18] J. Gea-Banacloche, Phys. Rev. Lett. **65**, 3385 (1990); Phys. Rev. A **44**, 5913 (1991); S.J. Phoenix and P.L. Knight, *ibid.* **44**, 6023 (1991); P.L. Knight and B.W. Shore, *ibid.* **48**, 642 (1993).

[19] T. Wong, O.E. Müstecaplıoğlu, L. You, and M. Lewenstein, Phys. Rev. A **62**, 033608 (2000).